ELSEVIER

Journal of Photochemistry and Photobiology A: Chemistry 94 (1996) 43–51

Journal of PHOTOCHEMISTRY AND PHOTOBIOLOGY A:CHEMISTRY

Aggregation of chlorophyll *b* in model systems

D. Frąckowiak [a,*], J. Goc [a], H. Malak [b], A. Planner [a], A. Ptak [a], B. Zelent [b]

[a] *Institute of Physics, Poznań University of Technology, Piotrowo 3, 60-965 Poznań, Poland*

[b] *Department of Biological Chemistry, School of Medicine, University of Maryland, 108 North Greene Street, Baltimore, MD 21201-1503, USA*

Received 25 October 1994; accepted 25 August 1995

Abstract

Chlorophyll *b* (Chl *b*) in model systems occurs in several forms. The relationship between these forms and the forms occurring in organisms is not yet clear. Chl *b* aggregation has been investigated less than that of Chl *a*. In this paper, several spectral features, e.g. fluorescence lifetimes in the picosecond time range, time- resolved delayed luminescence spectra, photoacoustic spectra and photopotential generation of Chl *b* embedded in model systems (poly(vinylalcohol) film or nematic liquid crystal), were measured.

The decay of the fluorescence of Chl *b* in polymer films can be analyzed, to a good approximation, on the basis of the following three exponential components: 3300–4300 ps, 400–900 ps and 40–71 ps. These decays are tentatively related to the emission of "dry" monomers and dry and wet dimers and oligomers respectively. The delayed luminescence spectra of the same samples in the microsecond range (at 8–295 K) are located in a similar spectral range to the fluorescence spectra. The intensity ratio between the delayed luminescence and prompt fluorescence is higher in the long-wavelength region, in which the oligomer emission is observed, than in the short-wavelength region, in which the emission of monomers and small aggregates predominates. The yield of thermal deactivation of the aggregated forms is higher than that of the monomers. The differences between the lifetimes of the various forms can be explained by the competition between the emission of prompt fluorescence, thermal deactivation and energy trapping (which is, in part, later deactivated as delayed luminescence).

The excitation energy transfer from "dry" monomers to aggregated forms is not very effective. The most effective process of excitation trapping followed by delayed luminescence emission occurs in oligomers of Chl *b*. On the basis of photopotential generation, the delayed luminescence is due, at least in part, to pigment ionization followed by slow charge recombination. The kinetics of photopotential generation and decay depend on the aggregation of the pigment.

Keywords: Chlorophyll *b*; Fluorescence lifetime; Delayed luminescence; Dye aggregation; Polymer film; Nematic liquid crystal; Photoacoustic spectra; Photopotential generation

1. Introduction

Chlorophyll *b* (Chl *b*) plays an important role as an antenna pigment of several photosynthetic organisms [1]. A knowledge of the interactions of Chls with macromolecules as well as the state of aggregation in various environments may be helpful in understanding the function of these pigments in organisms. Therefore the properties of Chls in various model systems have been widely investigated [2–12]. In most cases, the features of Chl *a* have been described. Chl *b*, which exhibits different aggregation properties from those of Chl *a* [13–15], has been investigated in less detail. The model of Chl *a* dimers has been proposed [9], whereas the structure of the small aggregates of Chl *b* has not been elucidated [16]. It is known that Chl *b* aggregation in "dry" [14,15] and "wet" [16] solvents is different. Poly(vinylalcohol) (PVA) film is a matrix in which both "dry" and "wet" forms of Chls are present [13], whereas in nematic liquid crystals (LCs) predominantly "dry" forms with a low degree of aggregation are observed [17–21].

On the basis of previous results [22], Chl *a* and Chl *b* at a concentration of 10^{-4} mol l^{-1} in PVA film form large oligomers which can be observed under a fluorescence microscope. Chl *a* oligomer formation requires the participation of water molecules [6]. The average dimensions of these Chl oligomers depend on the pigment concentration, and are different for Chl *a* and Chl *b* located in the same matrix. In addition, the oligomer rigidity, checked by film mechanical deformation, is different for Chl *a* and Chl *b* [22]. At concentrations of the order of 10^{-4} mol l^{-1}, Chl *a* in PVA occurs predominantly as "monomers" and "hydrated dimers" [13,23]. In the same range of concentration, Chl *b* is aggregated differently from Chl *a*, as suggested by previous investigations in several model systems [14,24,25] and by in vivo

* Corresponding author. Tel.: +48 61 782344; fax: +48 61 782324; e-mail: dfrackowiakpozn1v.tup.edu.pl.

SSDI 1010-6030(95)04201-6

investigations [21]. Previously [8,13], we have reported the emission lifetimes of Chls in PVA films measured in the nanosecond time region. The nanosecond emission involves, predominantly, prompt fluorescence excited by light absorption in molecules which are inefficient in excitation transfer to other pigment forms and in deactivation by other non-radiative pathways.

In this paper, we present, for Chl *b* in PVA, the fluorescence decay in the picosecond range. Such data provide information on the processes of excitation energy transfer between the various forms of Chl *b* and/or on other non- radiative pathways of de-excitation of the absorbed energy. We report the delayed luminescence (DL) of Chl *b* in PVA. The decay in the microsecond time range provides information on the energy trapped in the investigated system and emitted as DL. The photoacoustic spectra of the same sample enable the efficiency of thermal deactivation of the various forms of Chl *b* to be evaluated. Photopotential generation, investigated for Chl *b* in nematic LCs, indicates whether the illuminated pigment located in anisotropic surroundings can serve as an electron donor or electron acceptor, and whether the recombination of the ionized pigment occurs slowly in a time range comparable with the DL emission.

2. Materials and methods

Chl *b* was extracted from nettle leaves and column chromatographed on starch by the method described by Iriyama et al. [26]. An ether solution of the pigment was introduced into 20% (w/w) PVA–water solution and mixed until the ether had evaporated. The PVA–pigment viscous mixture was diluted with 10% (w/w) PVA–water solution to the appropriate pigment concentration and a film was prepared as described previously [27]. Two concentrations of Chl *b* in PVA film were prepared ($c_1 = 4 \times 10^{-5}$ mol l^{-1} and $c_2 = 1.3 \times 10^{-4}$ mol l^{-1}).

In order to prepare samples in LCs, an ether solution of purified Chl *b* was evaporated in a stream of N_2 and the pigment was dissolved in an LC mixture: *N*-(4-ethoxybenzylidene)-4-butylaniline (EBBA) and *N*-(4-methoxybenzylidene)-4-butylaniline (MBBA) (weight proportion, 3 : 2). EBBA and MBBA (Aldrich Chemical Co.) were used without further purification. The following concentrations of Chl *b* in LC were prepared: 1.0×10^{-3} mol l^{-1}, 1.4×10^{-3} mol l^{-1} and 4×10^{-5} mol l^{-1}. The LC solutions of Chl *b* were placed in a photoelectrochemical cell. The construction of the cell has been described previously [28,29].

The fluorescence lifetimes were measured using a picosecond and nanosecond time-correlated single-photon-counting fluorometer at The Center for Fluorescence Spectroscopy, University of Maryland, Baltimore, MD. The impulse response of this instrument was 50 ps full width at half-maximum (FWHM) with an MCP-PMT Hamamatsu R2809 red-sensitive detector. Excitation was achieved using pulses of 380 or 680 nm light with a pass duration of 5 ps. The source of light was obtained by pumping an Nd:YAG mode-locked laser (2 W at 532 nm, FWHM = 100 ps) and a Piridin 1 cavity-dumped dye laser (whose output was frequency doubled). The frequency repetition was 1 MHz. Fluorescence emission was detected at 660 ± 15 nm and 680 ± 15 nm using bandpass interference filters (Ditric Optics, Inc., Hudson, MA) or broad-band filters (RG-715, Andover Corporation, Salem, NH; Corning 7-60, Optical Products Dep., Corning, NY). Data were analyzed using IBH time-domain software (IBH Consultant, Ltd.).

Absorption spectra were measured with a Zeiss Specord M40; steady state fluorescence and DL time resolved spectra were obtained with apparatus constructed in Poznań.

The excitation light source in the DL apparatus consisted of a nitrogen and dye laser (type LD2C, PRA Laser Inc., Canada). The pulse duration was about 200 ps (FWHM). The intensity at the excitation wavelength was sufficiently low to avoid non-linear effects. The emission receiver was an R928 (Hamamatsu) photomultiplier operating in a single-photon-counting regime. Signals were collected in a multichannel analyzer (NTA-1024, version 4k, Works for Electronic Measuring Gear, Hungary) and computer processed. This apparatus has been described in detail elsewhere [30]. All DL spectra were taken with some additional delay (500 ns) with respect to the laser peak in order to eliminate the contributions from prompt fluorescence. This means that the photon-counting procedure was started with this "additional delay" with respect to the exciting laser peak. In order to measure DL at various temperatures, the sample was located in a cryostat (closed cycle refrigeration system, model TSL-22, Cryophysics SA, Switzerland). For anisotropic samples, the polarized light spectra were also taken.

The photoacoustic spectra were measured with a single-beam spectrometer as described previously [31,32].

Photopotentials were measured for Chl *b* solution in LCs located in an electrochemical cell [28,29]. The sample was sandwiched between semiconducting transparent electrodes and illuminated by a 75 W Xe lamp. The arrangement used for photopotential investigations has been described in detail previously [33].

3. Results

Fig. 1 presents the absorption spectra of Chl *b* in ether solution and in PVA film at two concentrations of the pigment. At the higher concentration ($c_1 = 1.3 \times 10^{-4}$ mol l^{-1}), in the film sample (curve 2), a band with a maximum at 465 nm predominates in the Soret band region, and in the red region, in addition to an absorption peak at 658 nm which is observed at the lower concentration, a new maximum at 630 nm appears. This shows that the pigment at higher concentration appears in an aggregated form contributing to the absorption bands at 465 and 680 nm. The positions of the absorption maxima of the various forms, evaluated from the absorption and fluorescence excitation spectra observed at

Table 1
Regions (nm) of fluorescence (F) and absorption or fluorescence excitation (A) of various forms of Chl *b* in model systems

	Matrix	"Dry" monomers or monomers interaction with matrix molecules	Small aggregates ("dry" and "wet")	Oligomers
F	PVA	653–658 [13], 655 [ts]	670–675 [ts]	670–710 [28], 710–740 [13], 756–760 [ts]
	LC	670 [24]		725, 735, 760 [24]
	Others	644–657 [15]	664 [13]	
A_{red}	PVA	650 [ts], 650 [13], 655 [24]	670 [ts]	635 [28], 680–685 [ts]
	LC	665 [ts]		
	Others	645 [16], 645 [34]	652 [15], 665 [16], 665 [34]	
A_{soret}	PVA	465 [ts], 467 [13], 468 [24]	416 [ts] ("dry"), 567–470 [ts]	450 [13], 465 [28]
	LC	470 [ts]		
	Others	457 [16], 460 [ts]	415 [15]	

[ts], data from this study.

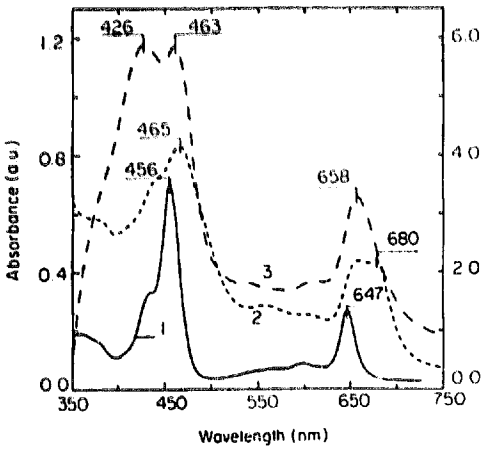

Fig. 1. Absorption spectra of Chl *b* in ethyl ether (curve 1) and PVA film (curve 2, $c_1 = 1.3 \times 10^{-4}$ mol l^{-1} (right scale); curve 3, $c_2 = 4 \times 10^{-5}$ mol l^{-1}) ($T = 295$ K).

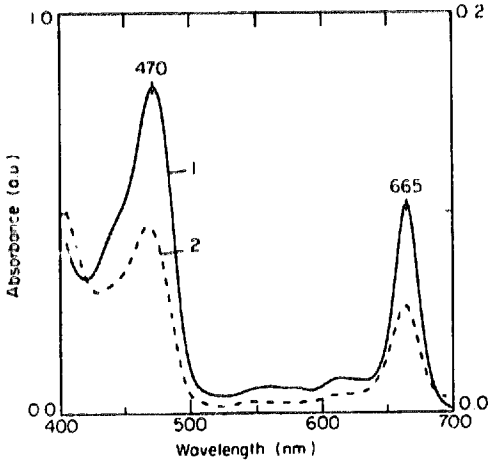

Fig. 2. Absorption spectra of Chl *b* in LC: curve 1, $c_1 = 1.0 \times 10^{-3}$ mol l^{-1}; curve 2, $c_2 = 1.4 \times 10^{-4}$ mol l^{-1} (right scale).

room and low temperatures and from the polarized excitation spectra (Figs. 4–6, see later), are given in Table 1. The Soret band of Chl *b* in both PVA samples is much broader than that in ether (Fig. 1), which is in agreement with the results obtained for Chl *a* bonded to macromolecules [35,36]. This shows that the aggregated forms of Chl *b* exhibit a much broader Soret band than the monodispersed pigment. From the ratio of the red to the Soret band in the absorption of the pigment in ether and PVA (Fig. 1), Chl *b* is not pheophytinized [37]. The change in band shape is therefore due to pigment aggregation.

The absorption of Chl *b* in LCs is shown in Fig. 2. The comparison of this spectrum with those reported previously [17–21] (Table 1) shows that, at both concentrations, the pigment is only aggregated to a low degree. It is practically in the monomeric state [21]. In nematic LCs, Chl *b* is strictly monomeric up to 10^{-3} mol l^{-1} because of the strong interaction with the solvent [24]. This monomeric form exhibits a fluorescence maximum at 670 nm. At much higher concentrations, maxima at longer wavelengths appear (725, 735 and 760 nm) [24]. This shows that, even in dry solvents, additional emission due to pigment interactions is observed. The absorption changes are not sufficiently large to explain (assuming a reasonable Stokes shift) the observed long-wavelength emission. Therefore it is expected that the observed emission is due to excimers. Excimers are easily formed in oriented samples at high pigment concentrations. The fluorescence measured at different frequencies of light modulation [14] shows that the emission in the 765 nm region is not monoexponential. This emission exhibits a very long lifetime (7 ns) due to the superposition of fluorescence with DL of these aggregated forms.

Fig. 3 shows the fluorescence spectra of PVA samples containing Chl *b*. The shape of the emission spectrum depends on the excitation wavelength and pigment concentration. At 380 nm excitation, used for lifetime measurements (curve 5), the emission intensities in the shorter wavelength region (600–700 nm) and longer wavelength region (about 750 nm) are comparable.

Fig. 4 shows the fluorescence excitation spectra of a PVA sample containing Chl *b* in four spectral regions: 655, 675, 700 and 760 nm (highly aggregated oligomers). In the Soret band region at 675 nm, the maximum at 416 nm predominates, but that at 467 nm is also well resolved. At 760 nm,

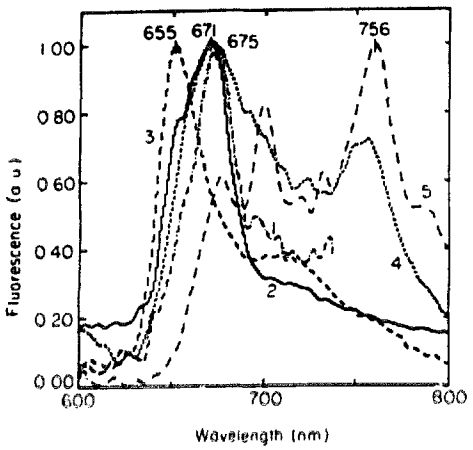

Fig. 3. Fluorescence spectra of Chl *b* in isotropic PVA (T = 295 K): curves 1–3, c_3; curves 4 and 5, c_1; 1, λ_{exc} = 380 nm; 2, λ_{exc} = 435 nm; 3, λ_{exc} = 425 nm; 4, λ_{exc} = 425 nm; 5, λ_{exc} = 380 nm.

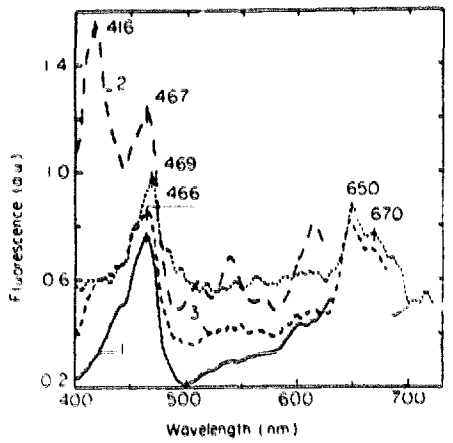

Fig. 4. Fluorescence excitation spectra of Chl *b* (c_3) in PVA at various regions of fluorescence observation: 1, 655 nm; 2, 675 nm; 3, 700 nm; 4, 760 nm.

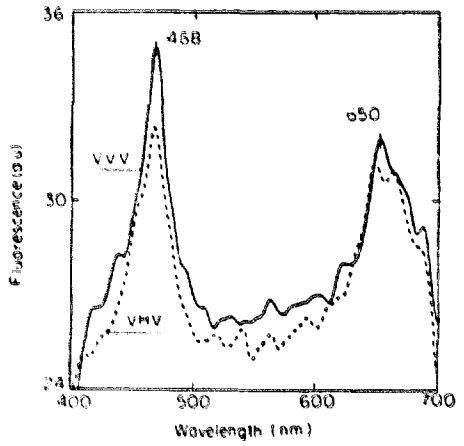

Fig. 5. Fluorescence excitation spectra of Chl *b* (c_1) in stretched PVA film for polarized VVV and VHV components (V, vertical; H, horizontal; the first and last letters refer to the polarization of the exciting and fluorescence light beams respectively, and the middle letter refers to the position of the stretching axis of the polymer matrix; T = 295 K).

the Soret maximum is located at 469 nm. In the Soret band, the excitation spectra of the various forms are better resolved than in absorption where all the components are hidden in the broad band located at 400–500 nm. This difference is due to the similar absorption coefficients of all Chl *b* forms, but the different efficiency of excitation of emission in the various spectral regions. In the red region of excitation, a broad band at 650–715 nm appears, in which, in addition to the main maximum at 650 nm, several long-wavelength shoulders can be seen. From Figs. 3 and 4, it follows that Chl *b* embedded in PVA film exhibits several emission bands: 655 nm, 670–675 nm and long-wavelength maxima differing in various samples (Table 1). The excitation band at 416 nm (Fig. 4) is probably due to similar "small dry aggregates" of Chl *b* as reported by Mazurek at al. [15]. The absorption in the red band region of several forms (monomers and small aggregates) probably overlaps giving a similar emission at about 670 nm. In PVA, at least two main forms (monomers and small aggregates) of Chl *b* are present and several highly aggregated clusters.

The ratio of the red to the Soret band depends on the wavelength of observation of fluorescence (Figs. 4 and 5), but in all cases this ratio is higher than in the absorption spectrum. This effect, also observed previously [38], is predominantly related to the various orientations of the absorption transition moments (TMs) of the different aggregated forms of Chl *b* with respect to the emission TMs of the observed fluorescence. This supposition is supported by the polarized fluorescence excitation spectra of stretched samples (Fig. 5). As a result of film stretching, various forms are differently reoriented changing the ratio of these bands. In addition, photoselection by polarized light influences the shape of the excitation spectrum, as observed by comparison of the VVV and VHV components (V, vertical; H, horizontal; the first and last letters refer to the polarization of the exciting and fluorescence light beams respectively, and the middle letter refers to the position of the stretching axis of the polymer matrix). The same conclusion can be obtained from the anisotropy coefficients of the excitation spectra, defined as $r_e = (VVV - VHV)/(VVV + 2VHV)$, which differ in the various spectral ranges. Values of the excitation emission anisotropy at the excitation maxima are $r_e(468) = 0.023$, $r_e(650) = 0.015$ and $r_e(664) = -0.001$. This shows that the various forms are differently oriented.

As can be seen in Fig. 6, a decrease in temperature changes the shape of the fluorescence excitation spectrum. This suggests that the equilibrium between various forms is shifted with a change in the sample temperature. Observations were made within the region of long-wavelength emission of the oligomers (760 nm). The contributions from all forms of Chl *b* can be distinguished in this spectrum, which shows that some transfer of excitation energy between the various forms of Chl *b* occurs. At low temperature, the excitation maximum at 685 nm predominates. This shows that the concentration of the aggregated form of Chl *b* absorbing at 685 nm increases

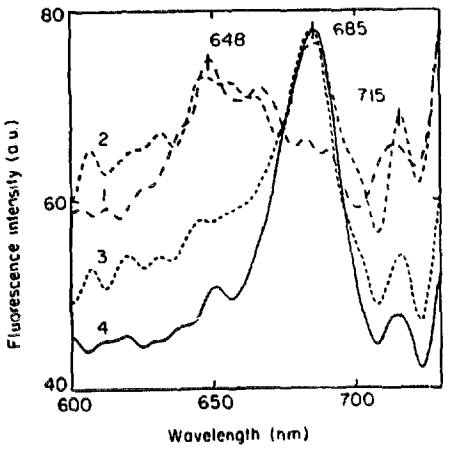

Fig. 6. Fluorescence excitation spectra (red part) of Chl *b* (c_1) in isotropic PVA at various temperatures. Observation of fluorescence at λ_{fl} = 760 nm; 1, 295 K; 2, 200 K; 3, 100 K; 4, 8 K.

at the expense of the other forms when the temperature is decreased.

In dry solvents, small aggregates are predominant [24]. In such systems at high concentration, the red band is shifted towards longer wavelengths and some structure appears [15]. The observed Stokes shift is much lower than usual for Chl *b* [37,39], suggesting the superposition of the absorption and emission of various "forms" with different fluorescence yields. The same conclusion can be drawn from the occurrence of structure in the red absorption band. A very low shift between the positions of the monomer and various aggregated forms in the red absorption range and in the emission spectra is very characteristic of dry solvents. The fluorescence band of Chl *b* in the solvents used reaches 655 nm at high concentrations, but this position depends strongly on the type of solvent. For example, Chl *b* in monolayers [13] exhibits a main fluorescence band at 664 nm.

Okada et al. [16] have investigated the aggregation of Chl *b* in hydrated solvents ("wet" sample according to Ref. [34]), and have found that the monomer and small aggregate absorption bands are located at 645 and 665 nm respectively. A model of the aggregates was not proposed, but the equilibrium between the monomers and small aggregates shifted with changing concentration. From a comparison of the results of Okada et al. [16] and Mazurek et al. [15], it can be concluded that "wet" aggregation causes a larger spectral shift of the red band than aggregation in a dry solvent. From a comparison of our data with the maxima of various forms reported in the literature (Table 1), we can see that the exact position of each maximum depends on the solvent used, but large differences are observed between aggregation in dry [14,15] and hydrated [16] solvents. In PVA, from previous results [13], "dry" and "wet" forms are present. From the well-resolved excitation spectra measured in the Soret band region (Fig. 4), two types of Chl *b* small aggregates can be proposed: "dry" with absorption at 416 nm, and "wet" with absorption at the long-wavelength side of Chl *b* monomers (470 nm). Monomer absorption is hidden between these two bands of dry and wet small aggregates, and it is not easy to establish its position.

Table 2 shows the data obtained from lifetime analysis. In all cases, analysis on the basis of three components provides the best fit. The analysis on the basis of different numbers of exponents is shown in Fig. 7. A monoexponential decay provides very high values of χ^2 (from 20 to 47), and therefore the values of τ obtained in this case are not shown in Table 2. Previously [13], the fluorescence decays measured for Chls in PVA in the nanosecond time range were also analyzed

Table 2
Fluorescence lifetimes (τ_i) of Chl *b* (c_1) in PVA films (analysis on the basis of two or three exponential components)

Sample	λ_{exc} (nm)	λ_{emis} (nm)	τ_1 (ps)	A_1 (%)	τ_2 (ps)	A_2 (%)	τ_3 (ps)	A_3 (%)	χ^2
U	380	660	3952±31	76	64±3	24	–	–	2.69
			4878±50	67	900±56	11	39.5±2.6	22	1.18
U	380	680	4302±40	72	76±4	28	–	–	2.79
			5233±54	65	716±38	10	42.8±1.9	25	1.17
U	380	>715	4353±190	20	75±3	80	–	–	5.81
			4809±930	16	632±60	9	55.7±2.7	75	1.38
U	680	760	2947±74	33	173±5	67	–	–	5.36
			4303±61	26	413±9	34	65.3±3.4	40	1.91
S	380	660	3487±34	75	156±6	25	–	–	4.23
			4265±34	64	637±21	18	46.5±3.4	18	1.08
S	380	680	3634±39	69	166±5	31	–	–	3.89
			4376±35	61	543±15	19	54.2±2.6	20	0.95
S	380	>715	3581±45	27	381±4	73	–	–	2.00
			3659±57	25	441±5	62	71.2±5.9	13	1.25
S	680	760	1521±43	39	86±9	61	–	–	5.99
			3305±63	20	484±11	32	30.3±2.5	48	1.88

U, unstretched films; S, 200% stretched films. A_i, amplitude contribution.

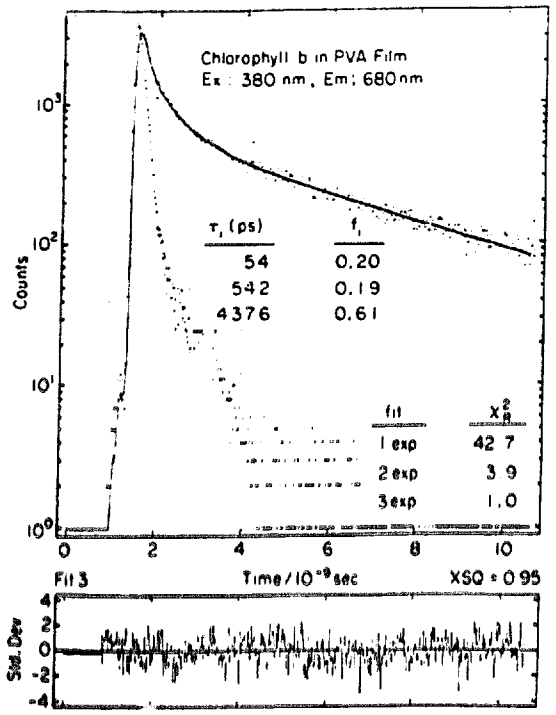

Fig. 7. Example of the decay curve of Chl *b* (c_1) in PVA: τ_i, lifetime of component; f_i, amplitude.

on the basis of three components. In the present set of measurements for Chl *b* in PVA, $\tau_1 \approx 3300$–4300 ps, $\tau_2 \approx 400$–900 ps and $\tau_3 \approx 40$–71 ps. The exact values depend on the wavelength of fluorescence excitation and emission. The fitting involves a mathematical procedure in which the amplitude and τ values of the components are varied. The analysis of strongly overlapping spectra cannot provide univocal values of the lifetime components without the application of global analysis [40]. Some information on the contributions to experimental decay from the various forms can be drawn from the τ values measured at various wavelengths of excitation and emission (Table 2).

From Table 2, it can be seen that, on excitation at 380 nm, which is absorbed by all forms [7,8,13,23], with observation of fluorescence in the long-wavelength region (oligomeric form region) ($\lambda > 715$ nm), a strong contribution from the shortest (60 ps) component is obtained; however, on excitation at the same wavelength with observation in the monomer region (at 660 nm), a large contribution from τ_1 (about 5000 ps) is observed, which must therefore be related to the "dry" monomer. A similar result is observed at 680 nm, since in this region the contribution from monomers is still strong; however, when the observation is shifted to 760 nm with excitation at 680 nm, the contribution from τ_2 (about 400 ps) increases. This component can be related to small aggregates. Film stretching causes an increase in the 400–500 ps component, suggesting an increase in emission of small aggregates as a result of film elongation. This indicates that the TMs of small aggregates exhibit a smaller angle with respect to the PVA plane in stretched than in isotropic films or that film stretching causes an increase in the concentration of this form. The contributions to τ from oligomers (τ_3) decrease as a result of film stretching. Therefore their TMs exhibit a larger angle with respect to the PVA plane in stretched than in isotropic films or their concentration decreases as a result of film deformation. The oligomer contribution (τ_3) increases when fluorescence observation at 760 nm is used.

Time-resolved DL spectra taken at various temperatures are shown in Fig. 8. Comparison of the prompt fluorescence spectrum corrected for photomultiplier sensitivity and analyzed on the basis of gaussian components with the similarly corrected and analyzed DL spectrum of the same sample shows that the oligomer contribution to DL is strong in comparison with that of small aggregates and monomers (Table 3). The ratio of the surface area under the gaussian component related to oligomers (maximum at 760 nm) to the sum of the surface areas of the short-wavelength gaussians belonging to small aggregates and monomers is equal to 1.4 for DL, but 0.69 for prompt fluorescence. The DL intensity is much lower than that of prompt fluorescence. The occurrence of the contribution to DL from all forms shows that all forms have their own traps. From Fig. 8, it can be seen that the DL intensity depends on the temperature. As a result of cooling of the sample to 100 K, the DL intensity is strongly increased

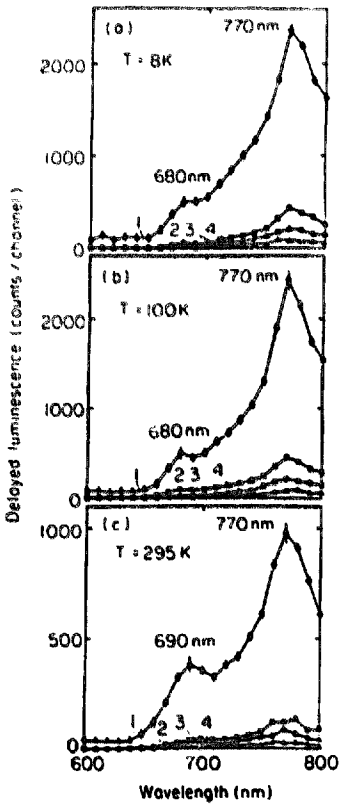

Fig. 8. Time-resolved delayed luminescence spectra of Chl *b* in isotropic PVA at various temperatures: (a) 290 K; (b) 100 K; (c) 8 K ($\lambda_{exc} = 425$ nm). Time windows: curve 1, 0.5–5.5 μs; 2, 5.5–10.5 μs; 3, 10.5–15.5 μs; 4, 20.5–25.5 μs.

and the DL of the aggregates with respect to the DL of other forms increases (Fig. 8).

The absorption and emission bands of all forms strongly overlap; therefore efficient excitation energy transfer between monomers and aggregated forms can be expected. Because of this strong overlapping of the absorption spectra, it is not easy to select one form on excitation. Variation in the excitation wavelength changes the contributions to absorption due to the various Chl *b* forms. If we assume similar oscillator strengths of Chl *b* in all forms, the surface areas under the gaussian components of absorption are proportional to the number of absorbing Chl *b* molecules. In the oligomer emission region (760 nm), the excitation spectrum surface area of the component in the monomer region (648 nm) is comparable with the monomer concentration evaluated from absorption analysis. This suggests inefficient energy transfer from monomers to oligomers. In the case of efficient excitation energy transfer between these forms, a much longer τ_1 value than τ_2 would not be observed. Let us suppose for simplicity that all oligomeric forms can quench other forms. With this assumption, a comparison of the lifetime of the monomeric form of Chl *b* in PVA in the presence of "oligomeric quenchers" (τ(DA)) with that of Chl *b* (in dry solvent, e.g. ether) in the absence of "quenchers" (τ(D)) enables the yield of energy transfer (ϕ_{ET}) between monomers and aggregated forms to be evaluated since it is proportional to $(1-\tau(DA))/\tau(D)$. This yield of energy transfer from monomeric forms to all aggregated forms must be low because, in ether at low concentrations of Chl *b*, $\tau = 5100$ ps is usually obtained and the most reasonable value of the monomeric Chl *b* lifetime (Table 2) is about $\tau = 4900$ ps. Therefore the influence of energy transfer on the lifetime of the dry form can be neglected. The evaluation of quenching would be much more complicated if a different distribution of small aggregates in PVA was assumed, but the sequence of lifetimes (Table 2) shows that the monomeric form is not efficiently quenched by aggregates.

The photoacoustic spectrum of Chl *b* in PVA is shown in Fig. 9. On the basis of this spectrum, the ratio of thermal deactivation at 676 nm to that at 650 nm is equal to about 1.4. This shows that monodispersed and aggregated forms of

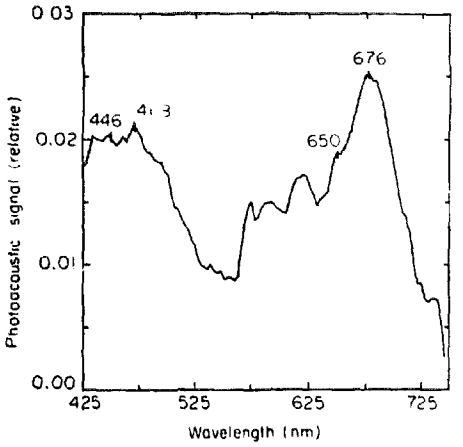

Fig. 9. Photoacoustic spectrum of Chl *b* (c_2) in PVA (frequency of light modulation, 7.75 Hz; phase shift between modulated light and acoustic wave, −120°).

Chl *b* differ in the amount of excitation lost as heat. In the Soret band, in the short-wavelength region, the photoacoustic spectrum cannot be measured because of the contribution from PVA. Some of the aggregated forms absorb in this region, and therefore the thermal deactivation at 440–460 nm is much lower than that in the red band where the absorption of all forms is strongly superimposed. A comparison of Figs. 9 and 1 shows that the thermal deactivation yields of the various forms of Chl *b* are very different: they are higher for aggregated than for monomeric forms. Because of the low DL intensity, other paths of deactivation besides DL emission must compete with fluorescence in the case of small aggregates and oligomers. Therefore it cannot be excluded that excitation trapping is followed not only by DL emission but also by thermal deactivation of the trapped energy. Aggregates lose a larger proportion of excitation by conversion into heat than monomers.

Previously [23,30], we have established that the DL of Chl *a* in PVA and other solvents is due to the formation and recombination of radical pairs delayed by electron trapping and occurs without triplet state participation. It seems that the DL of Chl *b* has similar character.

Photopotentials were measured only for LC solution, because of technical problems with such measurements in

Table 3
Examples of gaussian resolution analysis of prompt fluorescence and delayed luminescence of Chl *b* (c_1) in PVA

Spectrum	T (K)	λ_{exc} (nm)	Monomer			Small aggregate			Oligomer		
			λ (nm)	Area (%)	H-W (cm^{-1})	λ (nm)	Area (%)	H-W (cm^{-1})	λ (nm)	Area (%)	H-W (cm^{-1})
Prompt fluorescence	295	425	676	39	0.70	702	20	0.54	760	41	0.75
		435	676	38	0.70	702	22	0.54	760	40	0.75
		380	676	34	0.70	702	25	0.54	760	41	0.75
Delayed luminescence	295	425	676	21	0.70	702	21	0.54	760	58	0.75
	100	425	676	8	0.41	702	19	0.54	760	73	0.75
	8	425	676	8	0.41	702	22	0.54	760	70	0.75

H-W, half-width.

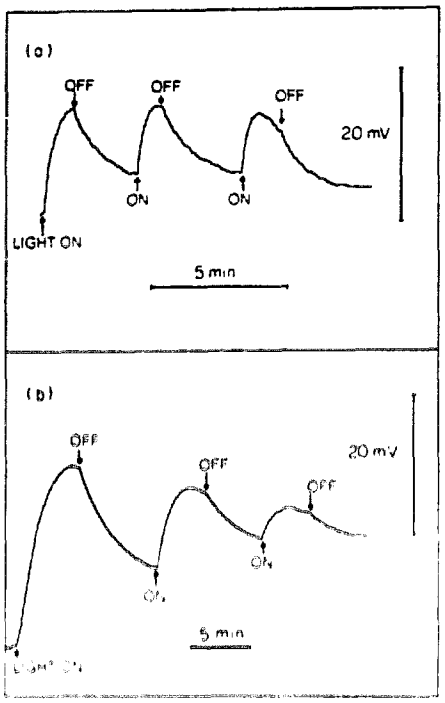

Fig. 10. Photopotential kinetics of Chl *b* in LC cell: (a) $c_1 = 1.0 \times 10^{-3}$ mol l^{-1}; (b) $c_1 = 4 \times 10^{-5}$ mol l^{-1}.

the case of PVA film [28]. The electrochemical cell filled with unpigmented LC does not exhibit measurable photopotentials. Even at very low pigment concentrations (10^{-5} mol l^{-1}), photopotentials are generated (Fig. 10). The photopotential kinetics depend on the pigment concentration. The absorption spectra (Fig. 2) show strong interaction of the pigment molecules with LC giving similar maxima shifts as observed previously [17–21]. The positions of the maxima are only slightly shifted with an increase in pigment concentration, indicating a low content of ground state aggregates of the pigment. The influence of the pigment concentration on the photopotential, as well as previous results suggesting efficient formation of pigment excimers in LC solutions [41], suggest the participation of excimers in photopotential generation. This may be confirmed by further experiments, but on the basis of Fig. 10 we can conclude that Chl *b* in anisotropic systems can serve as an electron donor. This supports our mechanism of DL generation.

The results presented show that the aggregation properties of Chl *b* differ strongly from those of Chl *a*. Chl *b* can form several, slightly different (in terms of their spectral properties) complexes with medium molecules as well as pigment aggregates with and without water participation [6,15,16,42]. In the case of Chl *b*, both "dry" and "wet" dimers can take part in the formation of large oligomers. Large aggregates can trap the excitation energy more efficiently than monomers and small aggregates.

Acknowledgements

Fluorescence lifetimes were measured at the Center for Fluorescence Spectroscopy (CFS), University of Maryland, which is supported by grants from the National Science Foundation (DIR-8710401) and from the National Institutes of Health (RR08119). D. Frąckowiak, J. Goc, A. Planner and A. Ptak are grateful for financial support from the Poznań University of Technology (grant NR 62-093).

References

[1] H. Scheer, *Chlorophylls*, CRC Press, Boca Raton, Ann Arbor, Boston, London, 1991.
[2] E.J. van de Meent, M. Kobayashi, C. Erkelens, P.A. van Veelen, J. Amesz and T. Watanabe, *Biochim. Biophys. Acta, 1058* (1991) 356.
[3] Y. Koyama, Y. Umemoto and A. Akamatsu, *J. Mol. Struct., 146* (1986) 237.
[4] Y. Koyama, Y. Umemoto, A. Akamatsu, K. Uehara and M. Tanaka, *J. Mol. Struct., 146* (1986) 273.
[5] K. Uehara, M. Mimuro and M. Tanaka, *Photochem. Photobiol., 53* (1991) 371.
[6] A. Agostiano, P. Cosma and M. Della Monica, *J. Photochem. Photobiol. A: Chem., 58* (1991) 201.
[7] G. Munger, R.M. Leblanc, B. Zelent, A.G. Volkov, M.I. Gugeshashvili, J. Galant, H.A. Tajmir-Riahi and J. Aghion, *Thin Solid Films, 210/211* (1992) 739.
[8] B. Zelent, J. Gallant, A.G. Volkov, M.I. Gugeshashvili, G. Munger, H.A. Tajmir-Riahi and R.M. Leblanc, *J. Mol. Struct., 297* (1993) 1.
[9] K. Uehara, Y. Hioki and M. Mimuro, *Photochem. Photobiol., 58* (1993) 127.
[10] S.S. Brody, *Z. Naturforsch., Teil C, 37* (1982) 260.
[11] M. Kaplanova and K. Vacek, *Photochem. Photobiol., 20* (1974) 371.
[12] S. Hoshina, *Biochim. Biophys. Acta, 638* (1981) 334.
[13] D. Frąckowiak, B. Zelent, A. Helluy, M. Niedbalska, J. Goc and R.M. Leblanc, *J. Photochem. Photobiol. A: Chem., 69* (1992) 213.
[14] J. Szurkowski, *Stud. Biophys., 125* (1988) 63.
[15] M. Mazurek, B.D. Nadolski, A.M. North, M.-Y. Park and R.A. Pethrick, *J. Photochem., 19* (1982) 151.
[16] K. Okada, K. Uehara and Y. Ozaki, *Photochem. Photobiol., 57* (1993) 958.
[17] D. Frąckowiak, S. Hotchandani and R. Leblanc, *Photobiochem. Photobiophys.*, 6 (1983) 339.
[18] D. Frąckowiak, J. Szurkowski, S. Hotchandani and R.M. Leblanc, *Mol. Cryst. Liq. Cryst., 111* (1984) 359.
[19] D. Frąckowiak, S. Hotchandani and R.M. Leblanc, *Photobiochem. Photobiophys., 7* (1984) 41.
[20] D. Frąckowiak, D. Bauman, H. Manikowski, W.R. Browett and M.J. Stillman, *Biophys. Chem., 28* (1987) 101.
[21] D. Wróbel and M. Kozielski, *Biophys. Chem., 33* (1989) 127.
[22] B. Zelent, J. Goc and R.M. Leblanc, *Curr. Top. Biophys., 17* (1993) 40.
[23] D. Frąckowiak, A. Planner and J. Goc, *Photochem. Photobiol., 58* (1993) 737.
[24] D. Frąckowiak, J. Szurkowski, B. Szych, S. Hotchandani and R.M. Leblanc, *Photobiochem. Photobiophys., 12* (1986) 9.
[25] R.L. van Metter, *Biochim. Biophys. Acta, 462* (1977) 642.
[26] K. Iriyama, N. Ogura and A. Takamiya, *J. Biochem., 76* (1974) 901.
[27] K. Fiksiński and D. Frąckowiak, *Spectrosc. Lett., 13* (1980) 873.
[28] D. Frąckowiak, M. Romanowski, S. Hotchandani, L. Leblanc, R.M. Leblanc and I. Gruda, *Bioelectrochem. Bioenerg., 19* (1988) 371.
[29] J. Goc and D. Frąckowiak, *J. Photochem. Photobiol. A: Chem., 59* (1991) 233.
[30] A. Planner and D. Frąckowiak, *Photochem. Photobiol., 54* (1991) 445.
[31] D. Ducharme, A. Tessier and R.M. Leblanc, *Rev. Sci. Instrum., 50* (1979) 42.

[32] D. Frąckowiak, A. Dudkowiak, B. Zelent and R.M. Leblanc, *J. Fluorescence, 1* (1991) 225.
[33] D.Frąckowiak and A. Ptak, *Photosynthetica, 30* (1994) 553.
[34] A.G. Volkov, M.I. Gugeshashvili, M.D. Kandelaki, V.S. Markin, B. Zelent, G. Munger and R.M. Leblanc, *Proc. Soc. Photo-opt. Instrum. Eng., 1436* (1991).
[35] I. Inamura, H. Ochiai, K. Toki, S. Watanabe, S. Hikino and T. Araki, *Photochem. Photobiol., 38* (1983) 1, 37.
[36] B. Zelent, G. Munger, A. Helluy and R.M. Leblanc, *J. Photochem. Photobiol. A: Chem., 57* (1991) 375.
[37] J.C. Goedher, in L.P. Vernon and G.R. Seely (eds.), *Chlorophylls*, Academic Press, New York and London, 1966, p. 147.
[38] D. Frąckowiak, S. Hotchandani and R.M. Leblanc, *Photobiochem. Photobiophys., 6* (1983) 339.
[39] F.F. Litvin and V.A. Sineshchekov, in Govindjee (ed.), *Bioenergetics of Photosynthesis*, Academic Press, New York, San Francisco, London, 1975, p. 620.
[40] A.R. Holzwarth, *Photochem. Photobiol., 43* (1986) 707.
[41] D. Frąckowiak, B. Zelent, H. Malak, R. Cegielski, J. Goc, M. Niedbalska and A. Ptak, *Biophys. Chem., 54* (1995) 95.
[42] G.R. Seely and A.A. Rehms, *Photochem. Photobiol., 55* (1992) 257.